Agricultural and Forest Meteorology 232 (2017) 35–47

Contents lists available at ScienceDirect

Agricultural and Forest Meteorology

journal homepage: www.elsevier.com/locate/agrformet

Analysis and estimation of tallgrass prairie evapotranspiration in the central United States

Pradeep Wagle[a,*,1], Xiangming Xiao[a,b], Prasanna Gowda[c], Jeffrey Basara[d], Nathaniel Brunsell[e], Jean Steiner[c], Anup K.C[f]

[a] Department of Microbiology and Plant Biology, and Center for Spatial Analysis, University of Oklahoma, Norman, OK 73019, USA
[b] Institute of Biodiversity Science, Fudan University, Shanghai 200433, China
[c] USDA-ARS Grazinglands Research Laboratory, El Reno, OK 73036, USA
[d] School of Meteorology and Oklahoma Climatological Survey, University of Oklahoma, Norman, OK 73019, USA
[e] Department of Geography and Atmospheric Science, University of Kansas, Lawrence, KS 66045, USA
[f] Department of Natural Resource Ecology and Management, Oklahoma State University, Stillwater, OK 74078, USA

ARTICLE INFO

Article history:
Received 14 September 2015
Received in revised form 6 August 2016
Accepted 8 August 2016

Keywords:
Artificial neural network
Eddy covariance
ET modeling
Empirical model
Remote sensing
Wavelet cross-correlation analysis

ABSTRACT

Understanding the factors controlling evapotranspiration (ET) of spatially distributed tallgrass prairie is crucial to accurately upscale ET and to predict the response of tallgrass prairie ecosystems to current and future climate. The Moderate Resolution Imaging Spectroradiometer (MODIS)-derived enhanced vegetation index (EVI) and ground-based climate variables were integrated with eddy covariance tower-based ET (ET_{EC}) at six AmeriFlux tallgrass prairie sites in the central United States to determine major climatic factors that control ET over multiple timescales and to develop a simple and robust statistical model for predicting ET. Variability in ET was nearly identical across sites over a range of timescales, and it was most strongly driven by photosynthetically active radiation (PAR) at hourly-to-weekly timescales, by vapor pressure deficit (VPD) at weekly-to-monthly timescales, and by temperature at seasonal-to-interannual timescales at all sites. Thus, the climatic drivers of ET change over multiple timescales. The EVI tracked the seasonal variation of ET_{EC} well at both individual sites ($R^2 > 0.70$) and across six sites ($R^2 = 0.76$). The inclusion of PAR further improved the ET-EVI relationship ($R^2 = 0.86$). Based on this result, we used ET_{EC}, EVI, and PAR (MJ m^{-2} d^{-1}) data from four sites (15 site-years) to develop a statistical model (ET = 0.11 PAR + 5.49 EVI − 1.43, adj. $R^2 = 0.86$, $P < 0.0001$) for predicting daily ET at 8-day intervals. This predictive model was evaluated against additional two years of ET_{EC} data from one of the four model development sites and two independent sites. The predicted ET ($ET_{EVI+PAR}$) captured the seasonal patterns and magnitudes of ET_{EC}, and correlated well with ET_{EC}, with R^2 of 0.87-0.96 and RMSE of 0.35-0.49 mm d^{-1}, and it was significantly improved compared to the standard MODIS ET product. This study demonstrated that tallgrass prairie ET can be accurately predicted using a multiple regression model that uses EVI and PAR which can be readily derived from remote sensing data.

1. Introduction

Evapotranspiration (ET) is a key component of the hydrologic cycle as approximately two-thirds of the precipitation received by the land surface is returned to the atmosphere via ET (Baumgartner et al., 1975) and it links atmospheric, hydrological, and ecological processes (Pielke et al., 1998). Understanding of the biological and climatic controls of ET has been a focus of climate change research for the past few decades (Brümmer et al., 2012). Currently, the eddy covariance (EC) technique is a widely used method for measuring ET at spatial scales of 100 s of meters (Baldocchi et al., 1988; Rana and Katerji, 2000) across temporal scales of hours to years (Baldocchi et al., 2001a). The concurrent measurement of climate variables at EC sites allows the examination of the driving factors that govern the variability of ET. Several studies have shown that ET is controlled by a number of climate variables such as solar radiation, air temperature (T_a), soil water content (SWC), vapor pressure deficit (VPD), and biological factors such as leaf emergence/development (Hu et al., 2009; Monteith, 1965; Priestley and Taylor, 1972; Stoy et al., 2006; Wagle et al., 2016a; Zha et al., 2010). Still, a lack of detailed information exists concerning cross-site vari-

* Corresponding author.
E-mail addresses: pradeep.wagle@ou.edu, pradeep.wagle@okstate.edu (P. Wagle).
[1] Current address: USDA-ARS Grazinglands Research Laboratory, El Reno, OK 73036, USA.

http://dx.doi.org/10.1016/j.agrformet.2016.08.005
0168-1923/

ability in ET and its response to major climatic factors at multiple timescales within widely distributed tallgrass prairie, a native and largely distributed ecosystem across central North America and considered a unique grassland unmatched elsewhere in the world (Changnon et al., 2002). Currently, it is the most endangered ecosystem in North America, occupying less than 4% of its pre-settlement area (~60 million ha) (Samson and Knopf, 1996). However, tallgrass prairie grasslands still provide habitat to support numerous grassland birds and other sensitive species, and contribute heavily for livestock production in several states of the United States. Thus, quantifying the extent to which ET varies in its response to climatic factors at multiple timescales within widely distributed tallgrass prairie ecosystems is crucial to move beyond site-level ET measurements to realistic estimates of water budgets over large areas (*i.e.*, regions or continents) and to predict the responses of tallgrass prairie ecosystems to current and future climate. To interpret EC time series data and assess the contributions of processes over multiple timescales, wavelet cross-correlation analysis is a suitable quantitative tool (Katul et al., 2001). This current study performs the wavelet cross-correlation analysis to draw new insights on the response of ET from six widely distributed tallgrass prairie ecosystems across the central United States to common climatic drivers over multiple (hour-to-interannual) timescales.

As EC sites and networks are limited in spatial scale and cover only a small portion of the tallgrass prairie areas, it is necessary to develop reliable methods to estimate ET over large tallgrass prairie areas. Satellite remote sensing can complement the restricted coverage of the global land surface by ground-based observation networks. Consequently, satellite remote sensing is generally considered as the most promising tool to estimate ET over large areas (Gowda et al., 2008). Predicting ET from remote sensing data falls broadly into two approaches: i) physical models based on the surface energy balance (SEB) concept (Gillies et al., 1997) and ii) empirical or statistical models based on the relationship between ET, vegetation indices, and climate variables (Choudhury et al., 1994; Nagler et al., 2005a), and most recently based on parameterized ecosystem water use efficiency (EWUE) using enhanced vegetation index (EVI) (Wagle et al., 2016a). These physical and empirical approaches have been extensively reviewed previously (Cleugh et al., 2007; Kustas and Norman, 1999; Mu et al., 2007; Mu et al., 2011). In past two decades, several SEB models have been developed to estimate large-scale ET (Allen et al., 2007; Bastiaanssen et al., 1998; Roerink et al., 2000; Senay et al., 2013; Su, 2002). A recent study (Bhattarai et al., 2016) that evaluated five SEB models in a humid subtropical climate suggests that the performance of different SEB models could vary with varying climate, land cover types, and soil moisture conditions. In addition, relatively complex computation of several land surface variables and turbulent heat fluxes, and requirement of many parameters with detailed information can significantly affect the precise partitioning of energy components and consequently the reliability of ET estimates by SEB models when input data are not readily available (Liou and Kar, 2014). Thus, when ground-based data are available, the empirical approach is more robust and a suitable scaling tool rather than solving complex physical models (Glenn et al., 2008). In the empirical approach, vegetation indices are directly used in scaling ET rather than using them to compute several canopy properties to be used as parameters in physical models (Bonan, 1993; Glenn et al., 2007). Cleugh et al. (2007) used the Moderate Resolution Imaging Spectroradiometer (MODIS) remote sensing data and provided regional ET estimates for evergreen forest and tropical savanna in Australia using a Penman-Monteith approach (Monteith, 1965). Mu et al. (2007) revised the algorithm proposed by Cleugh et al. (2007) and produced the MOD16 global ET product (ET_{MOD16}) at 1 km spatial resolution for 109 million km^2 of global vegetated land areas at 8-day intervals using ground-based global meteorology and MODIS data. The ET_{MOD16} algorithm was further improved (Mu et al., 2011).

In the past decade, several studies have established the potential of using empirical/statistical methods derived from remotely sensed vegetation indices and EC data to extrapolate EC measurements of carbon and water vapor fluxes over large spatial scales (Cleugh et al., 2007; Jung et al., 2010; Nagler et al., 2005a; Nagler et al., 2005b; Papale and Valentini, 2003; Wylie et al., 2003; Yang et al., 2007; Yang et al., 2006; Zhou et al., 2008). Wylie et al. (2003) developed a statistical algorithm by combining normalized difference vegetation index (NDVI) and EC data over a sagebrush-steppe ecosystem to map regional carbon fluxes. Following the same approach, Nagler et al. (2005a,b) predicted ET using EVI and T_a for riparian vegetation of western rivers in the U.S., and thus, suggesting the potential of integrating EVI with ground-based climate variables for better estimates of ET. Based on these results, along with the results of our previous study (Wagle et al., 2014) that showed a strong correlation between tower-based gross primary production (GPP_{EC}) and EVI in three AmeriFlux tallgrass prairie sites, we hypothesized that a robust relationship could be established by integrating EVI and major climate variables with ET_{EC} of tallgrass prairie across the central United States to accurately estimate ET. The approach of developing statistical algorithms by combining remote sensing and ground-based climate data to estimate ET has not been applied to the tallgrass prairie. It is essential

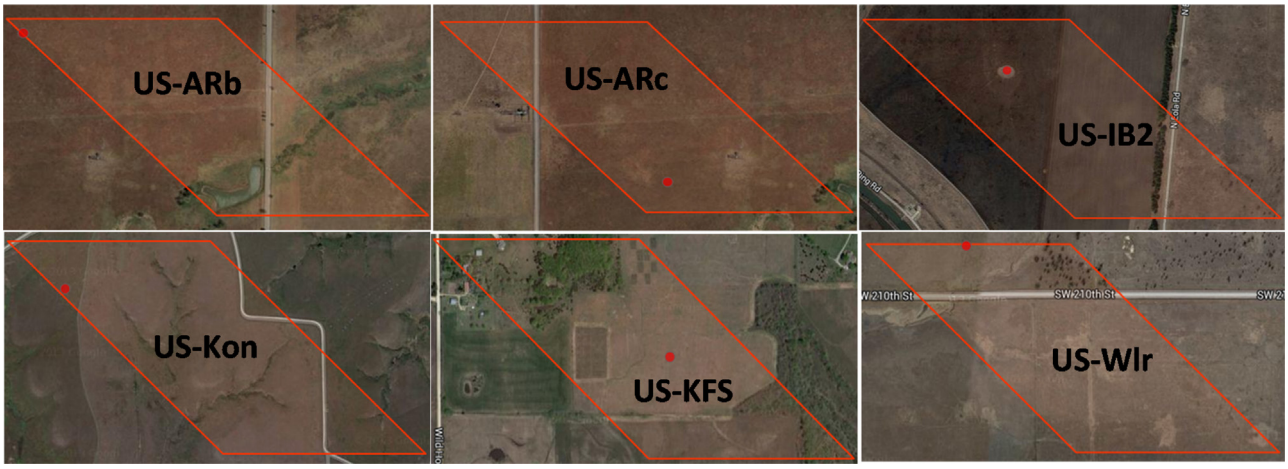

Fig 1. Landscapes of six AmeriFlux tallgrass prairie sites. The red boarder lines represent the size of one Moderate Resolution Imaging Spectroradiometer pixel (500 m spatial resolution) and the red dots represent the location of the flux towers (for interpretation of the references to colour in this figure legend, the reader is referred to the web version of this article).

Table 1
Site characteristics of six tallgrass prairie sites in this study.

Site (symbol)	Elevation (m)	Latitude	Longitude	Study period	Vegetation	Soil type	References
Model development sites							
El Reno burn, OK (US-ARb)	424	35.5497	−98.0402	2005–2006	C_4 dominated tallgrass prairie	Norge silt loam	Fischer et al. (2012)
El Reno control, OK (US-ARc)	424	35.5465	−98.0401	2005–2006	C_4 dominated tallgrass prairie	Norge silt loam	Fischer et al. (2012)
Fermi prairie, IL (US-IB2)	226	41.8406	−88.2410	2005–2009	C_4 dominated tallgrass prairie	Silt clay loam	Matamala et al. (2008)
Konza prairie, KS (US-Kon)	443	39.0824	−96.5603	2007–2012	C_4 dominated tallgrass prairie	Silt clay loam	Brunsell et al. (2008)
Model testing sites							
Fermi prairie, IL (US-IB2)	226	41.8406	−88.2410	2010–2011	C_4 dominated tallgrass prairie	Silt clay loam	Matamala et al. (2008)
Kansas Field Station, KS (US-KFS)	333	39.0561	−95.1907	2008–2012	C_3 dominated tallgrass prairie	Silt clay loam	Brunsell et al. (2014)
Walnut River, KS (US-Wlr)	408	37.5208	−96.8550	2002–2004	Tallgrass prairie (C_3/C_4 mixed)	Silt clay loam	Coulter et al. (2006)

Table 2
The coefficient of determination (R^2) for the relationships of tower-based evapotranspiration (ET_{EC}) with enhanced vegetation index (EVI), photosynthetically active radiation (PAR), and air temperature (T_a) at six tallgrass prairie sites. The highest R^2 value is highlighted in bold.

Site	EVI	PAR	T_a	EVI + PAR	EVI + T_a
US-ARb	0.84	0.72	0.74	0.91	0.88
US-ARc	0.84	0.61	0.76	0.90	0.89
US-IB2 (2005–2009)	0.78	0.81	0.79	**0.90**	0.83
US-Kon	0.71	0.70	0.72	**0.84**	0.79
Cross-site (model development dataset)	0.75	0.71	0.71	**0.86**	0.81
US-IB2 (2010–2011)	0.89	0.85	0.93	**0.96**	0.92
US-KFS	0.73	0.85	0.75	**0.90**	0.83
US-Wlr	0.86	0.77	0.77	**0.93**	0.90
Cross-site (model testing dataset)	0.80	0.76	0.70	**0.91**	0.84

Table 3
A comparison of performance of regression and artificial neural network (ANN) models for predicting evapotranspiration (ET) for four model development tallgrass prairie sites.

Model	Equation	R^2	AIC	SBC
PR	$-0.23 + 2.72\ EVI - 7.34\ EVI^2 + 0.30\ EVI \times PAR + 0.1\ EVI \times T_a$	0.88	−918.68	−896.29
MR1	$-1.28 + 5.01\ EVI + 0.09\ PAR + 0.01\ T_a$	0.86	−811.78	−793.87
MR2	$-1.43 + 5.49\ EVI + 0.11\ PAR$	0.86	−799.78	−786.34
MR3	$-0.57 + 5.55\ EVI + 0.05\ T_a$	0.81	−611.14	−597.70
LR	$-0.67 + 8.34\ EVI$	0.75	−437.93	−428.96
ANN			−915.34	−857.06

PR: polynomial regression; MR1: multiple regression with EVI, PAR, and T_a as predictors; MR2: multiple regression with EVI and PAR as predictors; LR: linear regression with EVI as a predictor; ANN: artificial neural network; R^2 = the coefficient of determination; AIC: Akaike's information criterion; and SBC: Schwarz's Bayesian criterion.

to develop reliable ET estimates over all land cover types for spatial water management and regional hydrological applications as ET estimates are used to derive several indices such as the crop water stress index (Jackson et al., 1981) or soil moisture index (Senay, 2008).

The objectives of this study were to (1) compare the magnitudes and seasonal patterns of ET_{EC} among six tallgrass prairie ecosystems, (2) investigate the properties of the power spectra of tallgrass prairie ET and its climatic forcing over multiple (hour-to-interannual) timescales across sites using wavelet cross-correlation analysis, and (3) develop a simple and robust statistical model for accurately predicting ET over large tallgrass prairie areas. Further, this study validates the standard MOD16 global ET product using ET_{EC} measured over tallgrass prairie ecosystems in the central United States.

2. Materials and methods

2.1. Site description

This study used six AmeriFlux tallgrass prairie sites located in the central United States that account for the majority of the available tallgrass prairie sites in the network. All six sites are situated in the same climate zone (*i.e.*, temperate continental climate; warm summer and long, cold, and snowy winter). An overview of the site characteristics is provided in Table 1, the landscape features of the study sites are shown in Fig. 1, detailed descriptions of the study sites can be found on the AmeriFlux website (http://ameriflux.ornl.gov/) or site-specific publications (Table 1).

2.2. Eddy covariance and ground-based climate data

Evapotranspiration at all study sites was measured using the EC technique. We acquired gap-filled Level-4 EC data and site-specific climate data such as T_a, SWC, VPD, photosynthetically active radiation (PAR), precipitation, and soil temperature (T_s) from the AmeriFlux data archive (http://ameriflux.ornl.gov/). Marginal Distribution Sampling (MDS) (Reichstein et al., 2005) and the Artificial Neural Network (ANN) (Papale and Valentini, 2003) methods are used to fill gaps in the AmeriFlux Level-4 data. The Level-4 data consists of ET with four different time steps: half-hourly, daily, 8-day, and monthly. The 8-day average values of ET and climate variables were used to match the temporal resolution of the MODIS-derived EVI. Further, we averaged ET_{EC}, T_a, and PAR data for the study period into a single composite year for each site to determine their mean seasonal patterns.

2.3. MODIS vegetation indices and the MODIS ET product (MOD16)

The 8-day composite MODIS land surface reflectance (MOD09A1) data for one MODIS pixel (500 m × 500 m) each

containing the coordinates of selected flux towers were downloaded from the MODIS data portal at the Earth Observation and Modeling Facility (EOMF), University of Oklahoma (http://eomf.ou.edu/visualization/). The MODIS pixels cover near uniform grassland conditions at most of the study sites (Fig. 1). However, due to the marginal fetch to the east at the US-IB2 site, the MODIS pixel included parcels of adjacent cropland (a strip of corn (*Zea mays* L.)/soybean (*Glycine max* L.) rotation) and native grassland. The MODIS pixel included some forest parcels at the US-KFS site and a small portion of shrubs at the US-Wlr site. We used surface reflectance (ρ) from blue, red, and near infrared (NIR) bands to compute EVI (Huete et al., 2002).

The global ET_{MOD16} data for the MODIS pixels surrounding each flux site were downloaded from the Oak Ridge National Laboratory Distributed Active Archive Center (ORNL DAAC) website (http://daac.ornl.gov/MODIS/modis.shtml).

2.4. Statistical analysis

To characterize the energetic frequencies/timescales of tallgrass prairie ET and also to relate them with the timescales of variability of major climate variables (T_a, T_s, PAR, VPD, and SWC), we relied on an orthogonal wavelet transformation with the Haar basis function. Non-gap filled ET and meteorological half-hourly time series data were normalized to have zero mean and unit variance, and were zero-padded to a length equal to the power of 2^{18} (2,62,144), greater than the length of the data record (up to 1,22,676 half-hourly data points) for any site in this study. We then determined and summed the wavelet coefficients within dyadic timescales ranging from 2^1 (hourly) to 2^{16} (~4 years) only as in previous studies (Novick et al., 2014; Stoy et al., 2005; Wagle et al., 2016c) since the wavelet coefficients associated with longer timescales (2^{17} or ~8 years) may not be reliable. A detailed description on applica-

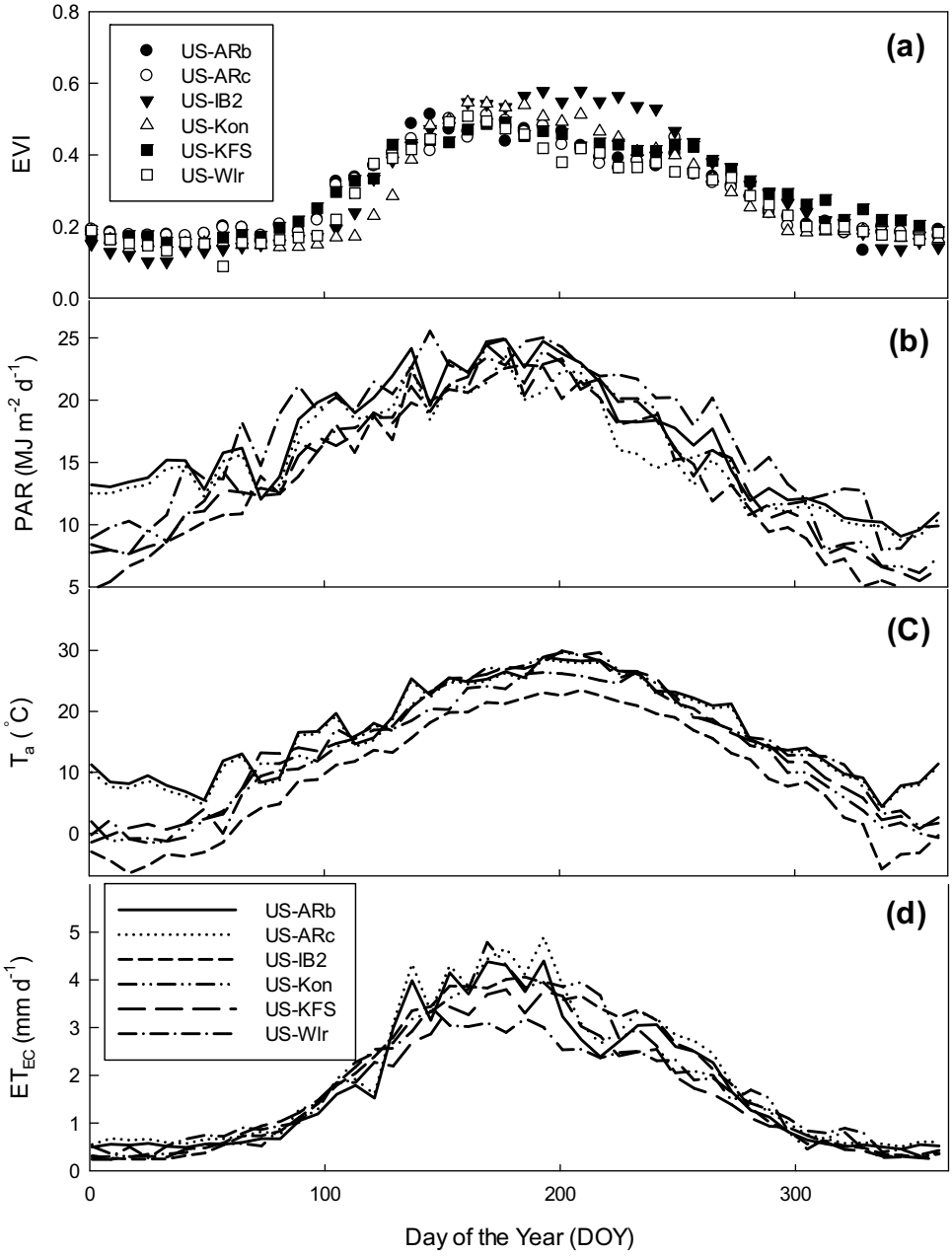

Fig. 2. Mean seasonal patterns (8-day composite) of enhanced vegetation index (EVI), photosynthetically active radiation (PAR), air temperature (T_a), and tower-based evapotranspiration (ET_{EC}) at six tallgrass prairie sites.

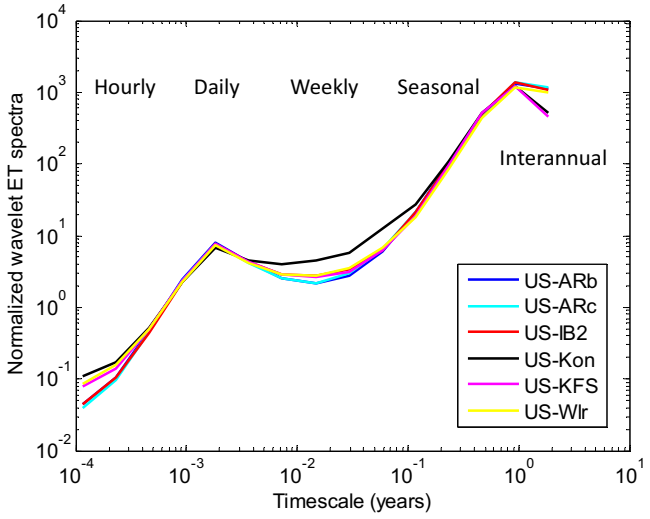

Fig. 3. Normalized wavelet spectra of evapotranspiration (ET, mm 30-min^{-1}) at six tallgrass prairie sites. Half-hourly data were used in the analysis.

tions of spectral analysis in fluxes can be found in previous studies (Baldocchi et al., 2001b; Katul et al., 2001; Torrence and Compo, 1998).

The ET_{EC} with EVI and climate variables (T_a, PAR, SWC, VPD, and precipitation) across all six tower sites were analyzed to determine if there was a significant correlation of ET_{EC} with EVI and climate variables. As such, various regression (simple, multiple, and polynomial) models were employed between ET_{EC} and major controlling variables at the four model development sites (15 site-years) to obtain the best predictive ET equation as follows:

$$ET = f(EVI, PAR, T_a \ldots) (1)$$

The stepwise selection method was used to select most significant variables. We examined correlations between most significant predictor variables (EVI, T_a, and PAR) to assess an issue of multicollinearity. If predictor variables show multicollinearity, the estimates of coefficients may vary from model to model, and correlations between pairs of predictor variables only may fail to provide detailed information on the linear dependence among predictor variables. Thus, we performed the variance inflation factor (VIF) test to detect the multicollinearity (Neter et al., 1996). The VIF value of 1 indicates no correlation among predictor variables, while the VIF value > 10 indicates a severe problem of multicollinearity. If the VIF value exceeds 4 then further investigation is required for the multicollinearity since multicollinearity may influence the least square estimations.

The predictive modeling technique, namely artificial neural network (ANN), was also applied to assess if it provides a better performance for predicting ET. Only those predictor variables identified as the most significant in the regression analysis were considered in ANN models. In this study, EVI and PAR were used as predictor variables to estimate ET in ANN. Several fit statistics such as regression slopes, the coefficient of determination (R^2), root mean squared error (RMSE), Akaike's information criterion (AIC), and Schwarz's Bayesian criterion (SBC) were used to evaluate the model performance and bias. We performed regression and ANN models in SAS Enterprise Miner 12.3 software (SAS Institute Inc., Cary, NC, USA).

Once the statistical model was developed, ET was predicted and evaluated against ET_{EC} data from two independent sites (US-KFS and US-Wlr) and additional two years (2010–2011) of data from the US-IB2 site. We also compared 8-day values of $ET_{EVI+PAR}$ and ET_{MOD16} with ET_{EC} to assess their relative performances.

Table 4
Annually or seasonally (DOY 97-297, in parentheses) integrated sums of tower-based (ET_{EC}) and modeled ($ET_{EVI+PAR}$) evapotranspiration at six tallgrass prairie sites. Over- or under-estimations by the model are presented in percentage (%).

Site	Year	ET_{EC} (mm)	$ET_{EVI+PAR}$ (mm)	%
US-ARb	2005	716 (615)	822 (640)	−14.89 (−4.08)
	2006	588 (510)	672 (539)	−14.39 (−5.78)
US-ARc	2005	789 (669)	768 (594)	2.65 (11.22)
	2006	647 (552)	618 (488)	4.49 (11.55)
US-IB2	2005[a]	607 (519)	575 (530)	5.26 (−2.24)
	2006[a]	495 (415)	548 (493)	−10.76 (−18.87)
	2007[a]	586 (535)	597 (555)	−1.87 (−3.86)
	2008[a]	675 (609)	583 (558)	13.66 (8.41)
	2009[a]	611 (538)	606 (548)	0.87 (−1.89)
	2010	713 (632)	691 (634)	3.07 (−0.35)
	2011	742 (665)	669 (617)	9.84 (7.20)
US-Kon	2007	661 (581)	613 (533)	7.17 (8.37)
	2008	684 (620)	610 (531)	10.79 (14.5)
	2009[a]	496 (433)	516 (428)	−4.0 (1.24)
	2010[a]	573 (492)	453 (380)	20.9 (22.78)
	2011[a]	485 (395)	546 (456)	−12.56 (−15.41)
	2012	598 (515)	567 (486)	5.13 (5.63)
US-KFS	2008	597 (515)	691 (581)	−15.72 (−12.86)
	2009	580 (512)	741 (618)	−27.87 (−20.71)
	2010	671 (578)	712 (610)	−6.15 (−5.44)
	2011	558 (486)	666 (566)	−19.21 (−16.40)
	2012	521 (429)	640 (537)	−22.82 (−25)
US-Wlr	2002	591 (506)	705 (570)	−19.25 (−12.65)
	2003	612 (519)	739 (613)	−20.73 (−18.12)
	2004[a]	590 (520)	677 (588)	−14.85 (−12.98)

DOY represents Day of the Year. 8-day ET_{EC} and $ET_{EVI+PAR}$ values were summed and multiplied by 8 to get annual or seasonal sums.
[a] ET measurements for some days were not available.

3. Results

3.1. Seasonal dynamics and magnitudes of EVI, PAR, T_a, and ET_{EC}

Similar seasonal trends and magnitudes of EVI, PAR, T_a, and ET_{EC} were observed across all six sites (Fig. 2); the maximum values of 8-day composite EVI ranged from 0.49 to 0.58, PAR ranged from 22.8 to 25.5 MJ m^{-2} d^{-1}, T_a ranged from 23.5 to 29.7 °C, and ET_{EC} ranged from 3.4 to 4.9 mm d^{-1}. Further, a close correspondence among EVI, PAR, T_a, and ET_{EC} patterns was observed across sites whereby (1) EVI and ET_{EC} increased rapidly at approximately DOY 100 with the greening up of the prairie vegetation, (2) reached a maximum during the plant maturity stage, and (3) declined with the beginning of vegetation senescence at ~DOY 300. Thus, the growing season for these prairie sites spanned approximately DOY 100 to DOY 300. Further, Fig. 1 shows that EVI was generally ≥0.20, PAR was ≥10 MJ m^{-2} d^{-1}, T_a was ≥5 °C, and ET_{EC} was ≥1 mm d^{-1} during the growing season.

3.2. Spectral characteristics of ET across sites

The normalized wavelet ET spectra were nearly identical at most timescales across sites, except at the US-Kon site at weekly-to-monthly timescales (Fig. 3), while the ET spectra slightly differed at hourly and interannual timescales among sites. The variability in ET was slightly larger at hourly and smaller at interannual timescales for the sites in Kansas. The wavelet cospectra of ET to major governing climate variables showed that variation in ET most resonated with PAR at hourly-to-weekly timescales, with VPD at weekly-to-monthly timescales, and with T_a and T_s at seasonal-to-interannual timescales at all sites (Fig. 4).

3.3. Controlling factors of ET_{EC}

We examined relationships of 8-day composite values of ET_{EC} with EVI and climate variables (PAR, T_a, SWC, VPD, and precipi-

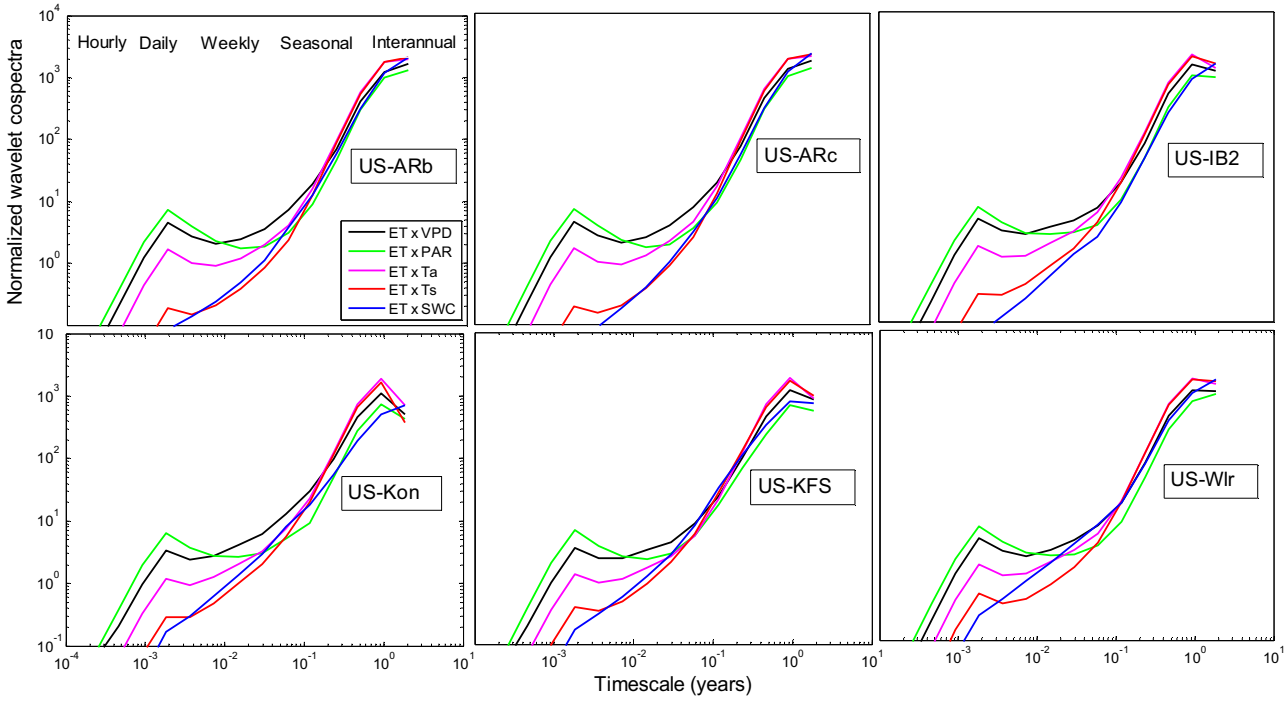

Fig. 4. Normalized wavelet cospectra of evapotranspiration (ET) with vapor pressure deficit (VPD), photosynthetically active radiation (PAR), air temperature (T_a), soil temperature (T_s), and soil water content (SWC) at six tallgrass prairie sites. Half-hourly data were used in the analysis.

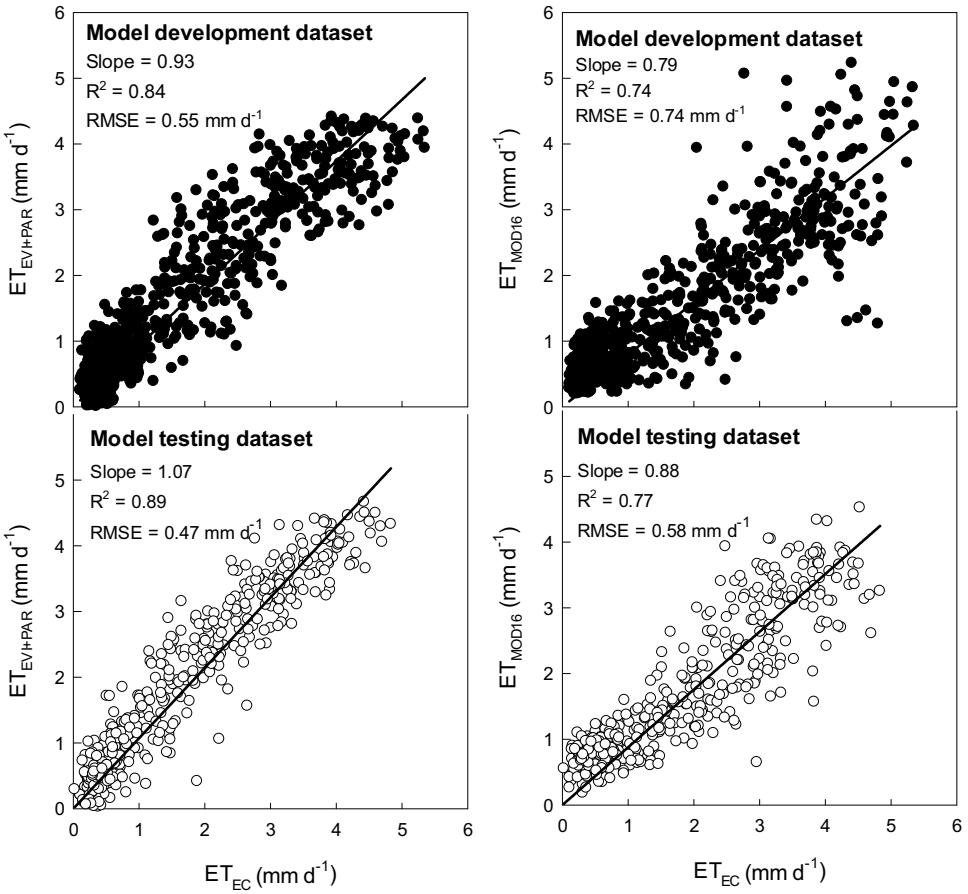

Fig. 5. A linear comparison of predicted ($ET_{EVI+PAR}$) and Moderate Resolution Imaging Spectroradiometer (ET_{MOD16}) evapotranspiration with tower-based evapotranspiration (ET_{EC}) across four model development and three model testing sites.

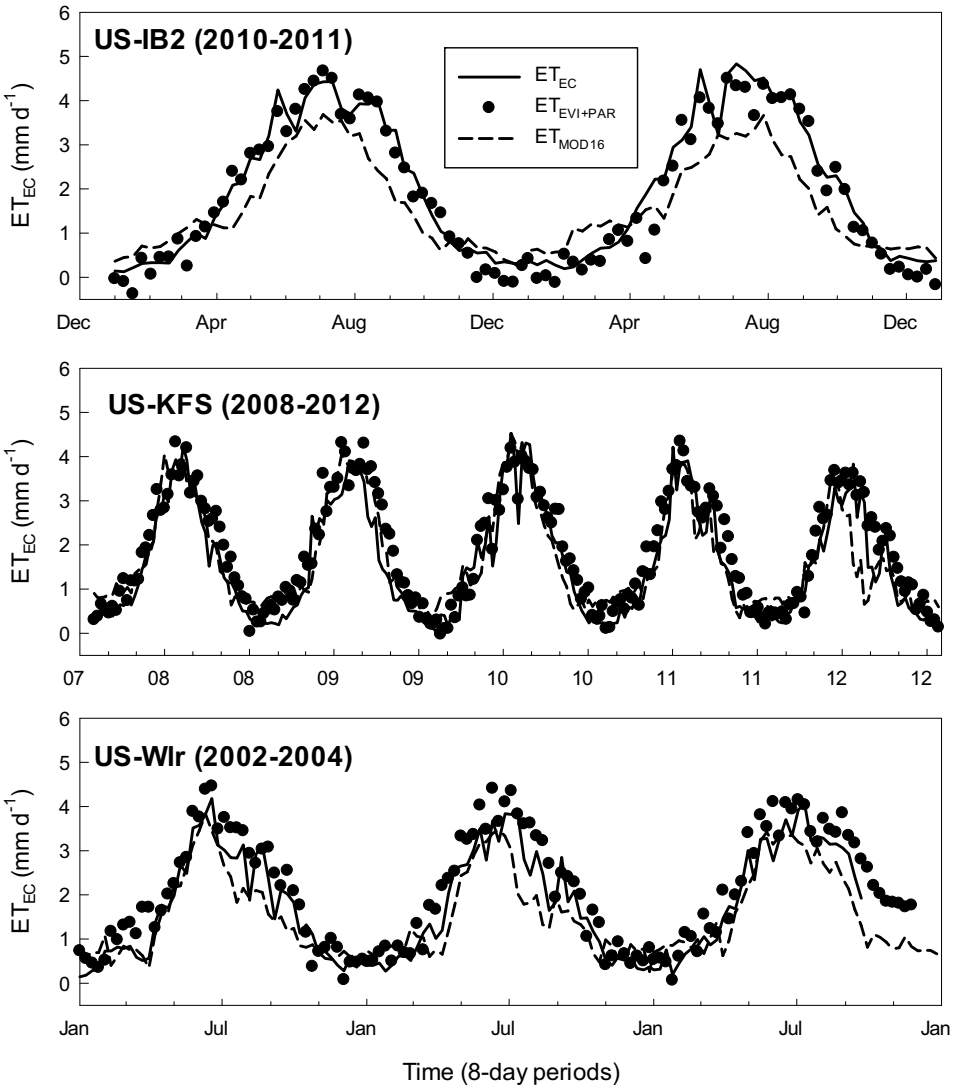

Fig. 6. A comparison of the seasonality and interannual dynamics (8-day composite) of predicted ($ET_{EVI+PAR}$), Moderate Resolution Imaging Spectroradiometer (ET_{MOD16}), and tower-based (ET_{EC}) evapotranspiration at three model testing sites.

tation). No meaningful relationships between ET and daily SWC or precipitation could be found (data not shown). The cross-site relationship showed that VPD explained only 48% of the variability in ET. Two most governing climate variables of ET were PAR and T_a at all six sites (Table 2). The results show that ET_{EC} was strongly correlated with EVI ($0.71 \leq R^2 \leq 0.89$), PAR ($0.61 \leq R^2 \leq 0.85$), and T_a ($0.72 \leq R^2 \leq 0.93$) at site levels. Integration of EVI with PAR or T_a further improved the ET-EVI relationship at all sites relative to EVI alone. In addition, EVI + PAR explained more variability in ET_{EC} than did EVI + T_a at all sites. Although the Pearson correlation coefficient (r) between EVI and PAR was 0.69 and between EVI and T_a was 0.77, VIF values were 2.45, 2.94, and 3.79 for EVI, PAR, and T_a, respectively. The results (VIF values < 4) suggested that multicollinearity between EVI and PAR, and between EVI and T_a was not an issue.

The cross-site analysis at the four model development sites showed that the proportion of the variability in ET_{EC} explained by EVI + PAR was 0.86, which was higher than that explained by either EVI + T_a (0.81) or EVI alone (0.75) (Table 3). The proportion of the variability in ET_{EC} explained by a polynomial regression (PR) using EVI, PAR, and T_a with interaction effects was 0.88, which was only 0.02 higher than that explained by a multiple regression (MR2) using EVI and PAR. The ANN model also did not improve the performance of predicting ET since the PR model had smaller AIC and SBC values than ANN (Table 3). Thus, for simplicity and parsimony, we selected a multiple regression (MR2 in Table 3) with EVI and PAR as predictors for predicting ET in this study.

3.4. Comparison between ET_{EC} and $ET_{EVI+PAR}$

Fig. 5 shows that predicted ET ($ET_{EVI+PAR}$) agreed well with ET_{EC} across the four model development sites (slope = 0.93, R^2 = 0.84, and RMSE = 0.55 mm d^{-1}) and three model testing sites (slope = 1.07, R^2 = 0.89, and RMSE = 0.47 mm d^{-1}). The seasonal trends and magnitudes of $ET_{EVI+PAR}$ also closely followed those of ET_{EC} at the three model testing sites (Fig. 6). A simple linear regression yielded high correlations between $ET_{EVI+PAR}$ and ET_{EC} at all three model testing sites (slopes = 0.95-1.14, R^2 = 0.87-0.96, and RMSE = 0.35-0.49 mm d^{-1}, Fig. 7). A comparison of annually or seasonally integrated ET_{EC} and $ET_{EVI+PAR}$ values also showed good agreement (Table 4). Integrated $ET_{EVI+PAR}$ values were within ±10-15% in most site-years. Slightly larger discrepancies between ET_{EC} and $ET_{EVI+PAR}$ were observed at US-KFS and US-Wlr sites where MODIS pixels included some forest/shrub parcels.

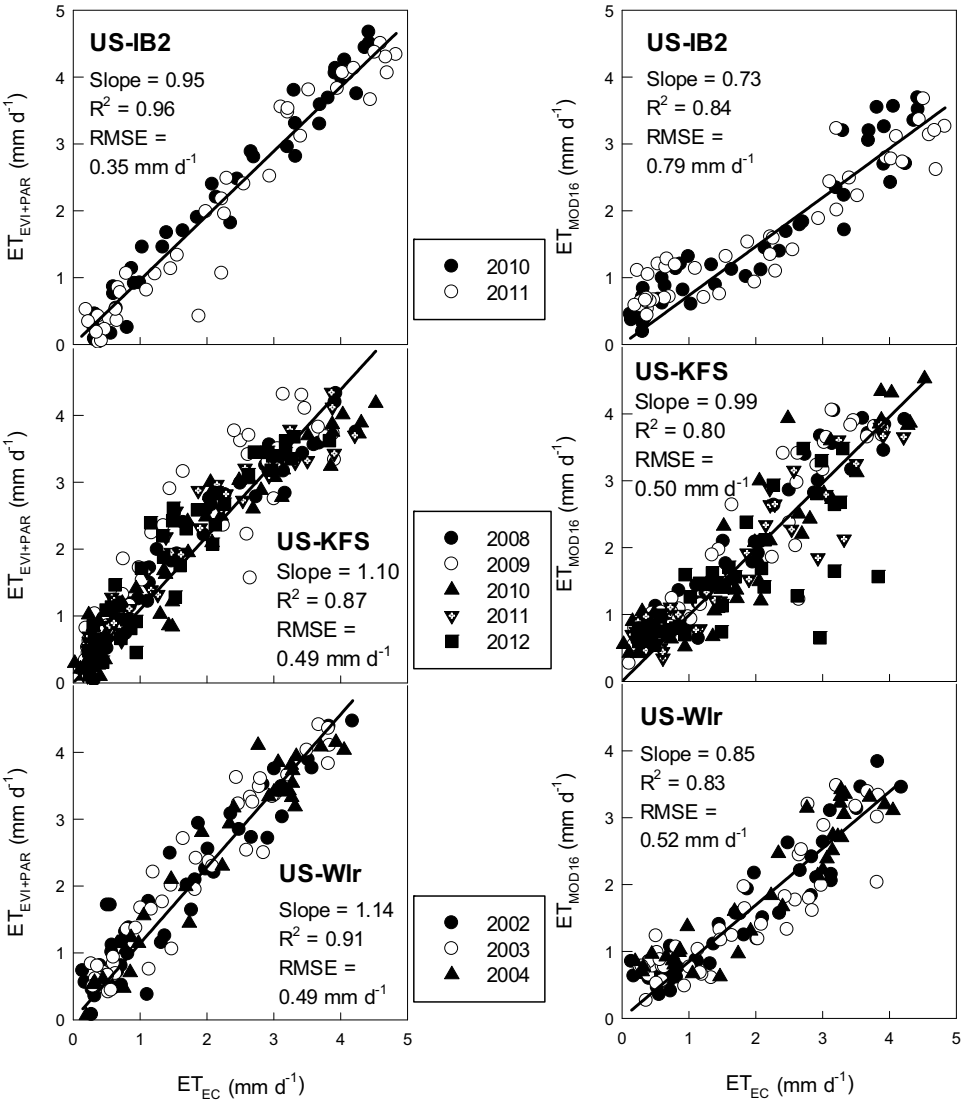

Fig. 7. A linear comparison of predicted ($ET_{EVI+PAR}$) and Moderate Resolution Imaging Spectroradiometer (ET_{MOD16}) evapotranspiration with tower-based evapotranspiration (ET_{EC}) at each of the three model development sites (different symbols for each year).

3.5. Comparison between ET_{EC} and ET_{MOD16}

Fig. 5 shows that ET_{MOD16} agreed well with ET_{EC} across the four model development sites (slope = 0.79, R^2 = 0.74, and RMSE = 0.74 mm d^{-1}) and three model testing sites (slope = 0.88, R^2 = 0.77, and RMSE = 0.58 mm d^{-1}). In general, the seasonal trends and magnitudes showed good correspondence between ET_{EC} and ET_{MOD16} at the three model testing sites (Fig. 6). A simple linear regression model showed high correlation between ET_{MOD16} and ET_{EC} at all three model testing sites (slopes = 0.73–0.99, R^2 = 0.80–0.84, and RMSE = 0.50–0.79 mm d^{-1}, Fig. 7). However, Figs. 5 and 7 show that R^2 values were relatively smaller and RMSE values were relatively larger for ET_{MOD16} than for $ET_{EVI+PAR}$.

4. Discussion

A strong relationship between seasonal patterns of EVI and ET_{EC} at both individual and across site levels indicated a strong linkage between vegetation canopy, as measured by EVI, and water use by tallgrass prairie. The cross-site ET_{EC}-EVI relationship on an eight-day timescale was further improved by coupling EVI with PAR (R^2 = 0.86) compared to coupling EVI with T_a (R^2 = 0.81) and EVI alone (R^2 = 0.75), indicating that EVI and PAR were main controlling factors of tallgrass prairie ET on that timescale. This result is further supported by the results of the wavelet cross-correlation analysis that PAR was the most important climatic driver of ET at hourly-to-weekly timescales (Fig. 4). Similar to our results, previous studies have also shown that ET is controlled by interaction between climatic and biological variables (Brümmer et al., 2012; Wilson and Baldocchi, 2000). Our results suggest that the observed day-to-day variation in ET was correlated more to variations in T_a and PAR than variations in SWC, VPD, and precipitation, which was consistent with findings for the day-to-day variation in net ecosystem CO_2 exchange (NEE) for a high-elevation, subalpine forest (Monson et al., 2002). Although NEE and ET processes are complex, and often controlled by phenological variability and variations in temperature, light intensity, and moisture availability, the diurnal cycles of irradiance and temperature dominate variations in NEE and ET on the diurnal timescale. For example, ET is lower during cloudy and cool periods than during sunny and warm periods.

A similar ET spectra (Fig. 3) and cospectra between ET and major climate variables (Fig. 4) indicated that variability in ET and climatic forcing of ET were nearly identical across sites over a range of timescales. The wavelet analysis provided some insights into how

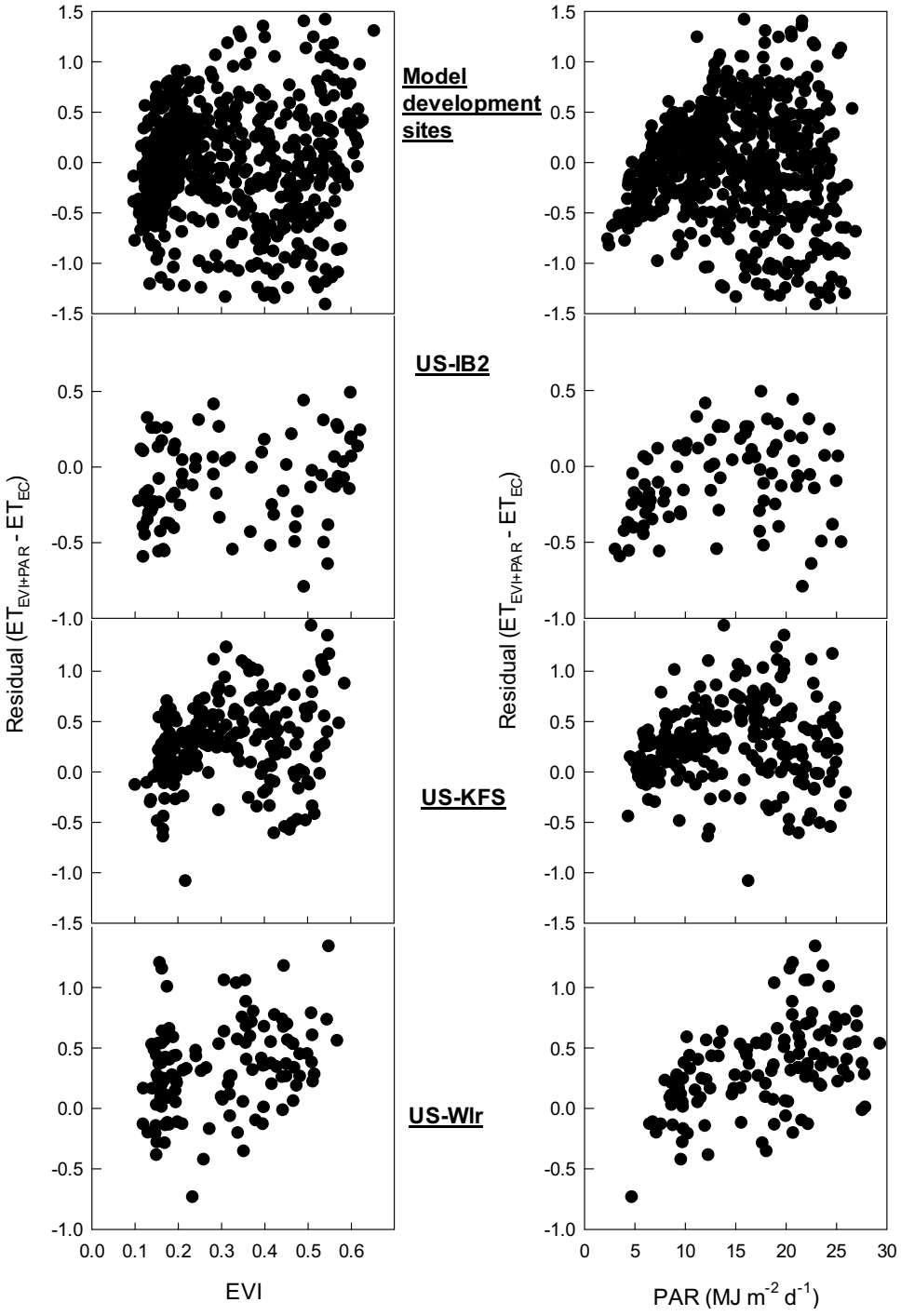

Fig. 8. Dependence of discrepancy in predicted ($ET_{EVI+PAR}$) and tower-based (ET_{EC}) evapotranspiration on enhanced vegetation index (EVI) and photosynthetically active radiation (PAR) across model development sites and at each of the three model testing sites.

the response of tallgrass prairie ET to environmental perturbations changes across various timescales. Our results show that no single climate variable was the most important driver of ET across a variety of timescales. Over shorter (hourly-to-weekly) timescales, PAR was the most important climatic driver of ET. This result is consistent with the findings of our previous studies (Wagle and Kakani, 2014; Wagle et al., 2016b) that not only reported a similar diurnal pattern of PAR and ET but also used strong linear relationships ($R^2 > 0.80$ in most cases) between half-hourly values of PAR and ET to fill gaps in ET at the weekly timescale in switchgrass (*Panicum virgatum* L.) and high biomass sorghum (*Sorghum bicolor* L. Moench). Synoptic weather changes that are associated with the passage of high and low pressure systems and fronts can impose weekly fluctuations in ET due to change in sky conditions, pressures, and humidity deficits (Baldocchi et al., 2001b). The wavelet analysis showed that VPD was the most important climate variable affecting tallgrass prairie ET at weekly-to-monthly timescales. Due to the seasonal change in sun's position, ecosystems experience changes in surface temperature and the amount of sun light received on seasonal scales (Baldocchi et al., 2001b). For this reason, T_a and T_s were most important climatic drivers of tallgrass prairie ET at longer (seasonal-to-interannual) timescales. It is important to note that

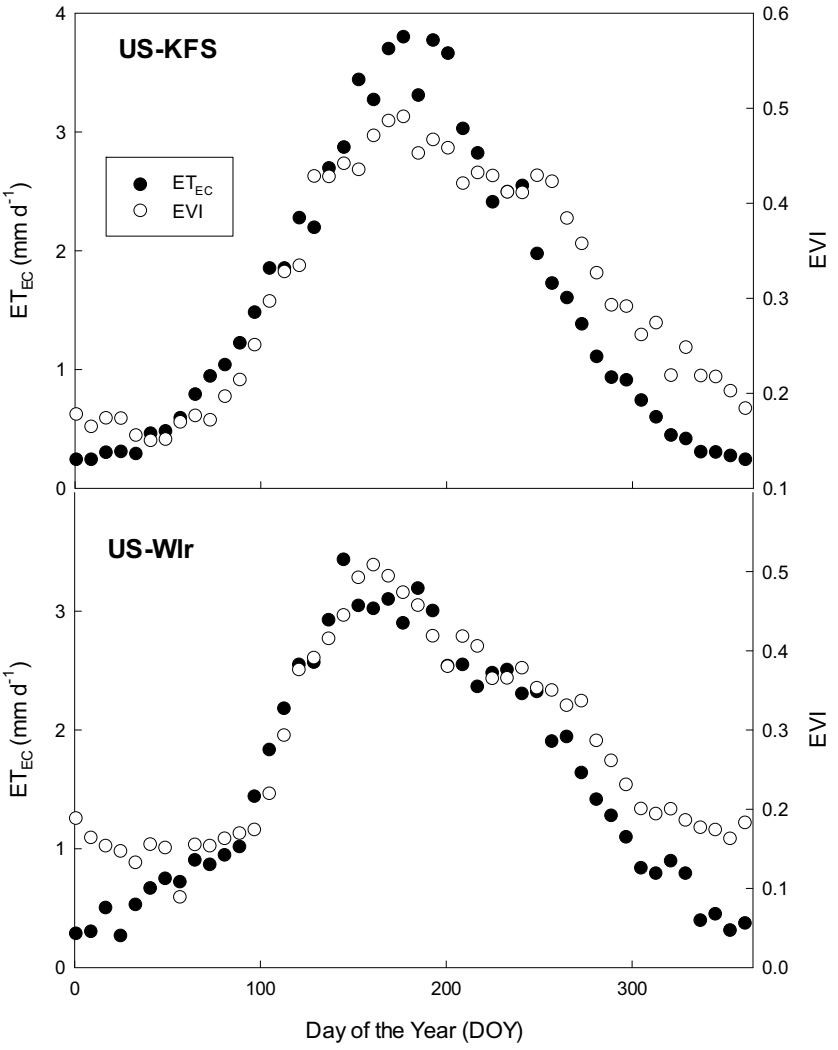

Fig. 9. A comparison of mean seasonal patterns (8-day composite) of tower-based evapotranspiration (ET_{EC}) and enhanced vegetation index (EVI) at US-KFS and US-Wlr sites.

different models operate at different (hour-to-annual) timescales. Our results illustrate that one should use different climatic drivers for different timescales for modeling purposes depending on the temporal resolution of models.

Multi-year and multi-site simulations of ET using EVI and PAR performed reasonably well for predicting the dynamics of tallgrass prairie ET. Our predicted ET was significantly improved compared to ET_{MOD16}. Previous studies have found mixed results such as over- or under-estimation and no or good relationships from comparison between ET_{MOD16} and ET_{EC} in a wide range of ecosystems (Kim et al., 2012; Mu et al., 2011; Ramoelo et al., 2014; Velpuri et al., 2013; Wagle et al., 2016a). Our results showed that the MODIS ET algorithm, in most cases, slightly underestimated ET at tallgrass prairie sites, but the ET_{MOD16} product successfully depicted the seasonal trends and magnitudes of ET_{EC} (Fig. 6), indicating the potential of the global ET_{MOD16} product to track tallgrass prairie ET.

Despite great correspondence between ET_{EC} and $ET_{EVI+PAR}$, large discrepancies still exist between them in a few 8-day periods (Fig. 6). These discrepancies can be partly attributed to multiple sources of errors or uncertainties. The first error source is the sensitivity of the predicted ET to its input parameters: EVI and PAR. To investigate the sensitivity of ET to EVI and PAR, ET residuals ($ET_{EVI+PAR} - ET_{EC}$) are plotted against EVI and PAR in Fig. 8. Results show that ET was slightly overestimated beyond PAR of 10 MJ m^{-2} d^{-1} at US-KFS and US-Wlr, while it was systematically underestimated at lower PAR levels (< 10 MJ m^{-2} d^{-1}) across the model development sites. The residuals did not show any systematic pattern against EVI across the model development sites, but ET was slightly overestimated at US-KFS and US-Wlr using EVI. This overestimation of ET at US-KFS and US-Wlr can be attributed to the earlier decline of ET_{EC} than EVI during the late growing season (Fig. 9), most likely because the MODIS pixel covers some forest parcels at US-KFS and a portion of shrubs at US-Wlr (Fig. 1); EVI is influenced by green forest/shrub canopies. In contrast, the flux tower footprint covered mostly grassland, and ET_{EC} declined rapidly after the senescence of grasses. When EC data are used for validation of remote sensing models, it is assumed that the EVI value for a MODIS pixel is representative for the EVI value for the flux tower footprint (especially short towers over croplands and grasslands). Our results demonstrate that the mismatch between the flux tower footprint and the MODIS pixel can contribute to some uncertainties in ET estimates, especially in case of surface heterogeneity within the MODIS pixel. Fig. 2 further supports that ET_{EC} was the lowest and EVI was the highest at US-KFS during the late growing season. When compared to other sites, clearly higher levels of PAR in spring and fall, and lower magnitudes of ET_{EC} in summer (Fig. 2) due to grazing could be attributed to overestimation of ET at US-Wlr. We further investigated the sensitivity of ET to wind speed at each of the three model

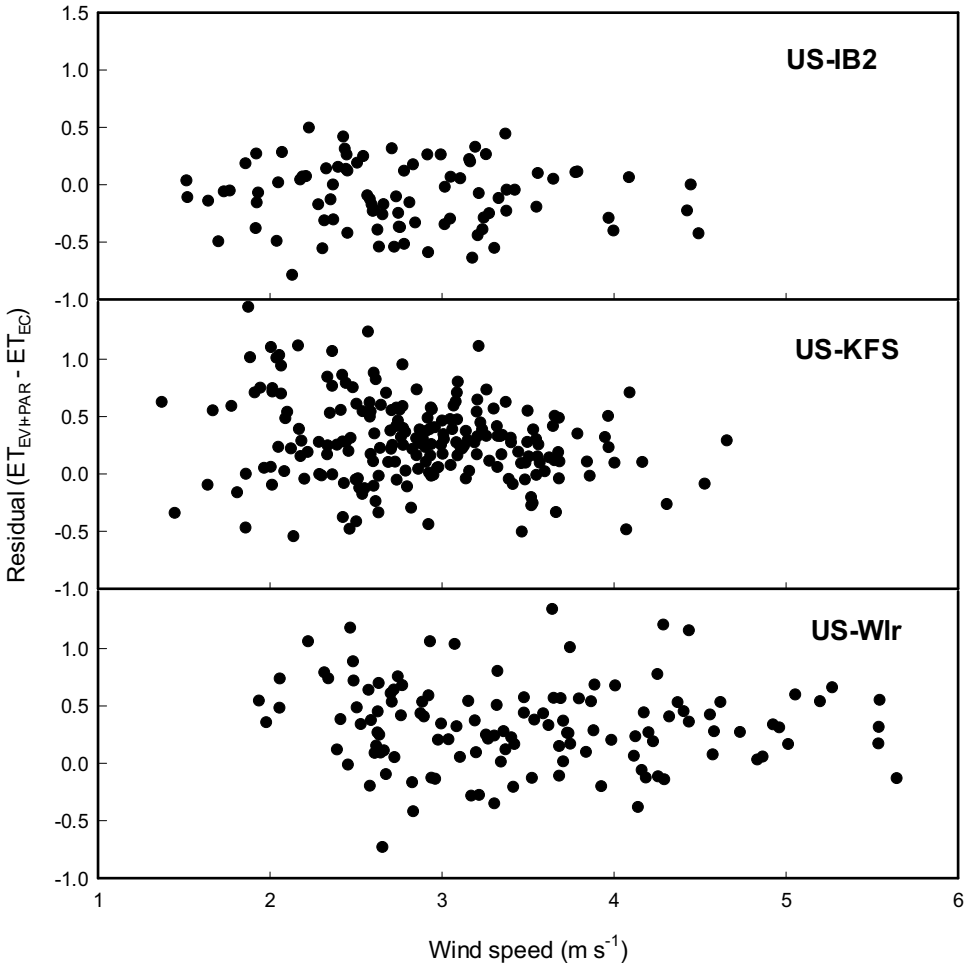

Fig. 10. Dependence of discrepancy in predicted ($ET_{EVI+PAR}$) and tower-based (ET_{EC}) evapotranspiration on wind speed at each of the three model testing sites.

testing sites (Fig. 10). Lack of any discernible trends of ET residuals to wind speed indicated that there were no systematic errors associated with wind speed. The second error source is the simplified assumptions that were made in estimating ET using only EVI and PAR, whereas EVI and PAR together explained 86% of the variations in ET_{EC} across the model development sites (Table 2). The representativeness of the limited AmeriFlux tallgrass prairie sites might have also presumably affected our ET estimation model. It is also important to note that the modeled and observed values cannot be identical even if all the modeling or observational errors or uncertainties could be reduced to zero (Taylor, 2001). The uncertainties in the large scale ET estimates from remote sensing data have been up to 50% of the average annual ET values (Mueller et al., 2011; Vinukollu et al., 2011). A reasonable upper limit of accuracy for the remote sensing based models to determine ET is approximately 20% (Jiang et al., 2004), indicating that our modeled ET results are within the reasonable agreement.

5. Conclusions

For a better understanding of the controlling factors of ET in tallgrass prairie ecosystems, we integrated ET_{EC} measurements with ground-based major climatic variables and the MODIS-derived EVI at six AmeriFlux tallgrass prairie sites. Variability in ET_{EC} was nearly identical across sites over a range of timescales. No single climate variable was the most important driver of ET across a variety of timescales, indicating that climatic forcing of ET changes over multiple timescales. At weekly timescale, EVI and PAR were two most important factors that control ET. Based on this result, we developed and evaluated a simple model that uses EVI and PAR as input data to predict ET at 8-day intervals. Our results demonstrate that the simple $ET_{EVI+PAR}$ model has the potential to provide estimates of tallgrass prairie ET with reasonable accuracy. This predictive model could be improved as more ET data becomes available from additional tallgrass prairie sites, and ultimately EVI and PAR could be sufficient to monitor tallgrass prairie ET over large areas. Our results can be further validated using independent tallgrass prairie flux sites. We accept that our specific parameterization for tallgrass prairie cannot be transferred to other ecosystems or regions, but the approach could be applied to develop a statistical model for predicting large-scale ET for other land cover types or regions.

Acknowledgements

This study was supported in part by a research grant (Project No. 2013-69002) through the USDA National Institute for Food and Agriculture (NIFA)'s Agriculture and Food Research Initiative (AFRI), Regional Approaches for Adaptation to and Mitigation of Climate Variability and Change, and a research grant (IIA-1301789) from the National Science Foundation EPSCoR. Flux and climate data were obtained from the AmeriFlux database (http://ameriflux.ornl.gov/). Data collection at the US-ARb and US-ARc sites was supported by the USDA-GRL and the Office of Biological and Environmental Research of the U.S. Department of Energy, Atmospheric Radiation Measurement Program, under contract No. DE-AC02-05CH11231. N.A.B. acknowledges support from the National Science Founda-

tion EPSCoR program (NSF EPS-0553722 and EPS-0919443) and the LTER program at the Konza Prairie Biological Station (DEB-0823341). In addition, the US-Kon and US-KFS Ameriflux sites are sponsored by the U.S. Department of Energy under a sub contract from DE-AC02-05CH11231. We would like to thank a reviewer and an Associate Editor Christoph Thomas for their thoughtful and constructive comments on the manuscript.

References

Allen, R.G., Tasumi, M., Trezza, R., 2007. Satellite-based energy balance for mapping evapotranspiration with internalized calibration (METRIC)—model. J. Irrig. Drain. Eng. 133 (4), 380–394.
Baldocchi, D.D., Hincks, B.B., Meyers, T.P., 1988. Measuring biosphere-atmosphere exchanges of biologically related gases with micrometeorological methods. Ecology 69 (5), 1331–1340.
Baldocchi, D., et al., 2001a. FLUXNET: a new tool to study the temporal and spatial variability of ecosystem-scale carbon dioxide, water vapor, and energy flux densities. Bull. Am. Meteorol. Soc. 82 (11), 2415–2434.
Baldocchi, D., Falge, E., Wilson, K., 2001b. A spectral analysis of biosphere-atmosphere trace gas flux densities and meteorological variables across hour to multi-year time scales. Agric. For. Meteorol. 107 (1), 1–27.
Bastiaanssen, W., Menenti, M., Feddes, R., Holtslag, A., 1998. A remote sensing surface energy balance algorithm for land (SEBAL). 1. Formulation. J. Hydrol. 212, 198–212.
Baumgartner, A., Reichel, E., Lee, R., 1975. The world water balance: mean annual global, continental and maritime precipitation, evaporation and run-off. Elsevier Scientific Publishing Company.
Bhattarai, N., Shaw, S.B., Quackenbush, L.J., Im, J., Niraula, R., 2016. Evaluating five remote sensing based single-source surface energy balance models for estimating daily evapotranspiration in a humid subtropical climate. Int. J. Appl. Earth Obs. Geoinf. 49, 75–86.
Bonan, G.B., 1993. Importance of leaf area index and forest type when estimating photosynthesis in boreal forests. Remote Sens. Environ. 43 (3), 303–314.
Brümmer, C., et al., 2012. How climate and vegetation type influence evapotranspiration and water use efficiency in Canadian forest, peatland and grassland ecosystems. Agric. For. Meteorol. 153, 14–30.
Brunsell, N.A., Ham, J.M., Owensby, C.E., 2008. Assessing the multi-resolution information content of remotely sensed variables and elevation for evapotranspiration in a tall-grass prairie environment. Remote Sens. Environ. 112 (6), 2977–2987.
Brunsell, N., Nippert, J., Buck, T., 2014. Impacts of seasonality and surface heterogeneity on water-use efficiency in mesic grasslands. Ecohydrology 7 (4), 1223–1233.
Changnon, S.A., Kunkel, K.E., Winstanley, D., 2002. Climate factors that caused the unique tall grass prairie in the central United States. Phys. Geogr. 23 (4), 259–280.
Choudhury, B.J., Ahmed, N.U., Idso, S.B., Reginato, R.J., Daughtry, C.S., 1994. Relations between evaporation coefficients and vegetation indices studied by model simulations. Remote Sens. Environ. 50 (1), 1–17.
Cleugh, H.A., Leuning, R., Mu, Q., Running, S.W., 2007. Regional evaporation estimates from flux tower and MODIS satellite data. Remote Sens. Environ. 106 (3), 285–304.
Coulter, R.L., et al., 2006. Surface energy and carbon dioxide fluxes above different vegetation types within ABLE. Agric. For. Meteorol. 136 (3-4), 147–158.
Fischer, M.L., et al., 2012. Carbon, water, and heat flux responses to experimental burning and drought in a tallgrass prairie. Agric. For. Meteorol. 166, 169–174.
Gillies, R., Kustas, W., Humes, K., 1997. A verification of the 'triangle' method for obtaining surface soil water content and energy fluxes from remote measurements of the Normalized Difference Vegetation Index (NDVI) and surface e. Int. J. Remote Sens. 18 (15), 3145–3166.
Glenn, E.P., Huete, A.R., Nagler, P.L., Hirschboeck, K.K., Brown, P., 2007. Integrating remote sensing and ground methods to estimate evapotranspiration. Crit. Rev. Plant Sci. 26 (3), 139–168.
Glenn, E.P., Huete, A.R., Nagler, P.L., Nelson, S.G., 2008. Relationship between remotely-sensed vegetation indices, canopy attributes and plant physiological processes: what vegetation indices can and cannot tell us about the landscape. Sensors 8 (4), 2136–2160.
Gowda, P.H., et al., 2008. ET mapping for agricultural water management: present status and challenges. Irrigation Sci. 26 (3), 223–237.
Hu, Z., et al., 2009. Partitioning of evapotranspiration and its controls in four grassland ecosystems: application of a two-source model. Agric. For. Meteorol. 149 (9), 1410–1420.
Huete, A., et al., 2002. Overview of the radiometric and biophysical performance of the MODIS vegetation indices. Remote Sens. Environ. 83 (1), 195–213.
Jackson, R.D., Idso, S.B., Reginato, R.J., Pinter, P.J., 1981. Canopy temperature as a crop water stress indicator. Water Resour. Res. 17 (4), 1133–1138.
Jiang, H., et al., 2004. The influence of vegetation type on the hydrological process at the landscape scale. Can. J. Remote Sens. 30 (5), 743–763.
Jung, M., et al., 2010. Recent decline in the global land evapotranspiration trend due to limited moisture supply. Nature 467 (7318), 951–954.
Katul, G., et al., 2001. Multiscale analysis of vegetation surface fluxes: from seconds to years. Adv. Water Resour. 24 (9), 1119–1132.
Kim, H.W., Hwang, K., Mu, Q., Lee, S.O., Choi, M., 2012. Validation of MODIS 16 global terrestrial evapotranspiration products in various climates and land cover types in Asia. KSCE J. Civ. Eng. 16 (2), 229–238.
Kustas, W.P., Norman, J.M., 1999. Evaluation of soil and vegetation heat flux predictions using a simple two-source model with radiometric temperatures for partial canopy cover. Agric. For. Meteorol. 94 (1), 13–29.
Liou, Y.-A., Kar, S.K., 2014. Evapotranspiration estimation with remote sensing and various surface energy balance algorithms—a review. Energies 7 (5), 2821–2849.
Matamala, R., Jastrow, J.D., Miller, R.M., Garten, C., 2008. Temporal changes in C and N stocks of restored prairie: implications for C sequestration strategies. Ecol. Appl. 18 (6), 1470–1488.
Monson, R.K., et al., 2002. Carbon sequestration in a high-elevation, subalpine forest. Glob. Change Biol. 8 (5), 459–478.
Monteith, J., 1965. Evaporation and the environment, the state and movement of water in living organisms. In: XIXth Symposium. Cambridge University Press, Swansea.
Mu, Q., Heinsch, F.A., Zhao, M., Running, S.W., 2007. Development of a global evapotranspiration algorithm based on MODIS and global meteorology data. Remote Sens. Environ. 111 (4), 519–536.
Mu, Q., Zhao, M., Running, S.W., 2011. Improvements to a MODIS global terrestrial evapotranspiration algorithm. Remote Sens. Environ. 115 (8), 1781–1800.
Mueller, B., et al., 2011. Evaluation of global observations-based evapotranspiration datasets and IPCC AR4 simulations. Geophys. Res. Lett. 38 (6).
Nagler, P.L., et al., 2005a. Predicting riparian evapotranspiration from MODIS vegetation indices and meteorological data. Remote Sens. Environ. 94 (1), 17–30.
Nagler, P.L., et al., 2005b. Evapotranspiration on western US rivers estimated using the Enhanced Vegetation Index from MODIS and data from eddy covariance and Bowen ratio flux towers. Remote Sens. Environ. 97 (3), 337–351.
Neter, J., Kutner, M.H., Nachtsheim, C.J., Wasserman, W., 1996. Applied Linear Statistical Models 4. Irwin, Chicago.
Novick, K.A., et al., 2014. On the difference in the net ecosystem exchange of CO2 between deciduous and evergreen forests in the southeastern United States. Glob. Change Biol., n/a–n/a.
Papale, D., Valentini, R., 2003. A new assessment of European forests carbon exchanges by eddy fluxes and artificial neural network spatialization. Glob. Change Biol. 9 (4), 525–535.
Pielke, R.A., et al., 1998. Interactions between the atmosphere and terrestrial ecosystems: influence on weather and climate. Glob. Change Biol. 4 (5), 461–475.
Priestley, C., Taylor, R., 1972. On the assessment of surface heat flux and evaporation using large-scale parameters. Mon. Weather Rev. 100 (2), 81–92.
Ramoelo, A., et al., 2014. Validation of global evapotranspiration product (MOD16) using flux tower data in the African savanna, South Africa. Remote Sens. 6 (8), 7406–7423.
Rana, G., Katerji, N., 2000. Measurement and estimation of actual evapotranspiration in the field under Mediterranean climate: a review. Eur. J. Agron. 13 (2), 125–153.
Reichstein, M., et al., 2005. On the separation of net ecosystem exchange into assimilation and ecosystem respiration: review and improved algorithm. Glob. Change Biol. 11 (9), 1424–1439.
Roerink, G., Su, Z., Menenti, M., 2000. S-SEBI: a simple remote sensing algorithm to estimate the surface energy balance. Phys. Chem. Earth Part B 25 (2), 147–157.
Samson, F.B., Knopf, F.L., 1996. Prairie Conservation: Preserving North America's Most Endangered Ecosystem. Island Press.
Senay, G.B., et al., 2013. Operational evapotranspiration mapping using remote sensing and weather datasets: a new parameterization for the SSEB approach. JAWRA J. Am. Water Resour. Assoc. 49 (3), 577–591.
Senay, G.B., 2008. Modeling landscape evapotranspiration by integrating land surface phenology and a water balance algorithm. Algorithms 1 (2), 52–68.
Stoy, P.C., et al., 2005. Variability in net ecosystem exchange from hourly to inter-annual time scales at adjacent pine and hardwood forests: a wavelet analysis. Tree Physiol. 25 (7), 887–902.
Stoy, P.C., et al., 2006. Separating the effects of climate and vegetation on evapotranspiration along a successional chronosequence in the southeastern US. Glob. Change Biol. 12 (11), 2115–2135.
Su, Z., 2002. The surface energy balance system (SEBS) for estimation of turbulent heat fluxes. Hydrol. Earth Syst. Sci. Discuss. 6 (1), 85–100.
Taylor, K.E., 2001. Summarizing multiple aspects of model performance in a single diagram. J. Geophys. Res.: Atmos. (1984–2012) 106 (D7), 7183–7192.
Torrence, C., Compo, G.P., 1998. A practical guide to wavelet analysis. Bull. Am. Meteorol. Soc. 79 (1), 61–78.
Velpuri, N.M., Senay, G.B., Singh, R.K., Bohms, S., Verdin, J.P., 2013. A comprehensive evaluation of two MODIS evapotranspiration products over the conterminous United States: using point and gridded FLUXNET and water balance ET. Remote Sens. Environ. 139, 35–49.
Vinukollu, R.K., Meynadier, R., Sheffield, J., Wood, E.F., 2011. Multi-model, multi-sensor estimates of global evapotranspiration: climatology, uncertainties and trends. Hydrol. Processes 25 (26), 3993–4010.
Wagle, P., Kakani, V.G., 2014. Growing season variability in evapotranspiration, ecosystem water use efficiency, and energy partitioning in switchgrass. Ecohydrology 7 (1), 64–72.
Wagle, P., et al., 2014. Sensitivity of vegetation indices and gross primary production of tallgrass prairie to severe drought. Remote Sens. Environ. 152 (0), 1–14.

Wagle, P., Gowda, P.H., Xiao, X., Kc, A., 2016a. Parameterizing ecosystem light use efficiency and water use efficiency to estimate maize gross primary production and evapotranspiration using MODIS EVI. Agric. For. Meteorol. 222, 87–97.
Wagle, P., Kakani, V.G., Huhnke, R.L., 2016b. Evapotranspiration and ecosystem water use efficiency of switchgrass and high biomass sorghum. Agron. J. 108 (3).
Wagle, P., et al., 2016c. Differential responses of carbon and water vapor fluxes to climate among evergreen needleleaf forests in the USA. Ecol. Process. 5 (1), 1–17.
Wilson, K.B., Baldocchi, D.D., 2000. Seasonal and interannual variability of energy fluxes over a broadleaved temperate deciduous forest in North America. Agric. For. Meteorol. 100 (1), 1–18.
Wylie, B.K., et al., 2003. Calibration of remotely sensed, coarse resolution NDVI to CO2 fluxes in a sagebrush-steppe ecosystem. Remote Sens. Environ. 85 (2), 243–255.
Yang, F., et al., 2006. Prediction of continental-scale evapotranspiration by combining MODIS and AmeriFlux data through support vector machine Geoscience and Remote Sensing. IEEE Trans. on 44 (11), 3452–3461.
Yang, F., et al., 2007. Developing a continental-scale measure of gross primary production by combining MODIS and AmeriFlux data through Support Vector Machine approach. Remote Sens. Environ. 110 (1), 109–122.
Zha, T., et al., 2010. Interannual variation of evapotranspiration from forest and grassland ecosystems in western Canada in relation to drought. Agric. Forest Meteorol. 150 (11), 1476–1484.
Zhou, G., et al., 2008. Estimating Forest Ecosystem Evapotranspiration at Multiple Temporal Scales with a Dimension Analysis Approach1. Wiley Online Library.